GL01151

DEPARTMENT OF GEOLOGY AND GEOPHYSICS

REPORT: FINAL: Volume 77-13

CONTRACT: EY-76-S-07-1601

AGENCY: DOE/DGE

TITLE: FLUID DYNAMIC PROPERTIES OF RHYOLITIC MAGMAS, MINERAL MOUNTAINS, UTAH
Part I: Volatile Content and Flow Characteristics
Part II: Physical Properties

AUTHORS: W. P. Nash and S. H. Evans, Jr.

DATE: July 1978

UNIVERSITY OF UTAH SALT LAKE CITY, UTAH 84112

FINAL REPORT: VOLUME 77-13

DOE/DGE

EY-76-S-07-1601

Fluid Dynamic Properties of Rhyolitic Magmas, Mineral Mountains, Utah

Part I: Volatile Content and Flow Characteristics

Part II: Physical Properties

by

W. P. Nash and S. H. Evans, Jr.

Department of Geology and Geophysics

University of Utah

Salt Lake City, Utah 84112

ABSTRACT

Part I describes rhyolites from southwestern Utah that display striking dissimilarities in morphology which are attributed to viscosity differences due to variations in water content. Temperature effects and fluorine concentrations are unable to account for the observed differences in morphology. Fluid dynamic calculations indicate that rhyolite flows of fluid aspect contained between 1 and 3 percent water upon eruption. More viscous domes contained less water which was expelled in pyroclastic eruptions preceeding emplacement of the domal rhyolite magma.

Part II presents the results of calculations that determine the physical properties of rhyolite magmas in the Mineral Mountains. Data are presented on density, molar volume, heat capacity, gram formula mass, dynamic viscosity, thermal conductivity, thermal diffusivity, kinematic viscosity, and coefficient of thermal expansion.

I. Volatile Content and Flow Characteristics

INTRODUCTION

Flows, air-fall and ash-flow deposits, and domes of Quaternary rhyolite were formed over a period of 0.8 to 0.5 million years ago in the Mineral Mountains of southwestern Utah. Although all of the rhyolite formations are very similar in chemical composition, the contrasting morphology of flows versus domes demonstrates that there were fundamental differences in the fluid characteristics of the magmas giving rise to each. We present here results which suggest that the differences between these two magma types are related to differing concentrations of volatile constituents, especially water. In this paper we describe the morphology of the flows and domes, their volatile components, and apply these data to simple models for the flow of natural silicic liquids.

Geologic summary

The Mineral Mountains constitute a large horst approximately 50 km in length by about 10 km at its maximum width. It is made up mostly of a large composite Tertiary granite pluton through which Quaternary rhyolite was erupted for 15 km along the crest and western flank of the mountain range. The earliest eruptions at 0.8 m.y. ago produced two extremely fluid rhyolite flows, whereas subsequent eruptions from 0.6 to 0.5 m.y. ago produced at least 10 rhyolite domes which were preceded by the eruption of air-fall and ash-flow tuffs. A general geologic summary is given by Ward et al. (1978), a description of the volcanic rocks is provided by Lipman et al. (1977), and a detailed study of the petrology and mineralogy is given

by Evans and Nash (1978).

Chemistry

Obsidian from the two early rhyolite flows is generally simiar in composition to obsidian from the younger domes. Chemical analyses of two representative obsidians are given in Table 1. Both lavas are high silica rhyolites (76.5%) and both contain over nine percent total alkalies, although flow rhyolites have a higher K_2O/Na_2O ratio. Obsidians from both types contain very little water, whereas they contain substantial amounts of fluorine, especially in the younger dome-forming magma (0.4%). Obsidian from rhyolite flows contains 1 to 5 percent phenocryst material, whereas, in the domes, phenocryst contents range from about 4 to 8 percent (Evans and Nash, 1978).

MORPHOLOGY

Cross-sections of flows and domes are shown in Fig. 1. The two flows, Bailey Ridge and Wildhorse Canyon, are atypical for rhyolite as they appear to have been very fluid. Maps of the two flows are given in Fig. 2. Each flow is approximately 3 km long and about 80 meters thick. The base of each flow consists of 3 to 5 meters of massive obsidian which grades upward into a well layered zone of alternating bands of devitrified rhyolite and massive obsidian. Gray, devitrified rhyolite makes up the interior of the flows. A 1 meter thick band of obsidian is present about 15 meters below the top surface of the flows. The uppermost portions of flows consist of perlite and pumiceous rhyolite. The presence of a gas phase is indicated by lithophysoidal cavities often concentrated in linear bands corresponding

TABLE 1

Chemical Analyses of Representative Rhyolites

Weight %	Bailey Ridge Flow 74-3A	N. Twin Flat Mountain Dome 75-20
SiO_2	76.52	76.45
TiO_2	0.12	0.08
Al_2O_3	12.29	12.79
Fe_2O_3	0.31	0.30
FeO	0.46	0.29
MnO	0.05	0.10
MgO	0.08	0.12
CaO	0.64	0.40
Na_2O	3.80	4.39
K_2O	5.24	4.73
P_2O_5	0.02	0.06
H_2O^+	0.12	0.10
H_2O^-	0.06	-
F	0.16	0.44
Sum	99.87	100.25
Less O=F	0.07	0.19
Total	99.80	100.06
ppm		
Ba	130	-
Ce	60	40
La	45	35
Rb	195	340
Sr	35	-
Zr	100	90
Nb	25	35

Fig. 1. Cross-sections of flows and domes of the Mineral Mountains. Most of the rhyolite has been erupted upon the erosional surface of a tertiary granite pluton although flows may extend out over alluvium.

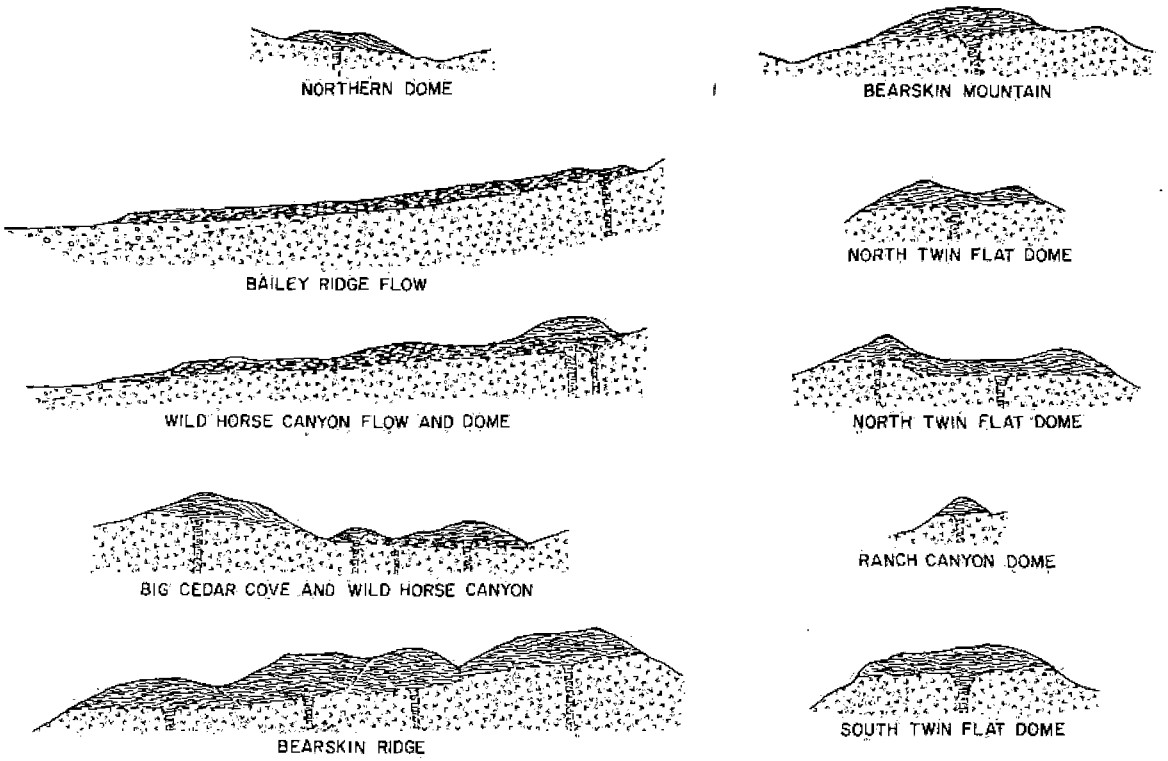

MINERAL RANGE VOLCANICS

SCALE 1:24000

1 1/2 0 1 MILE

1000 0 1000 2000 3000 4000 5000 6000 7000 FEET

.5 0 1 KILOMETER

Fig. 2. Geologic maps of flow rhyolites. Symbols in rhyolite indicate the strike and dip of flow layering (after Evans, 1977).

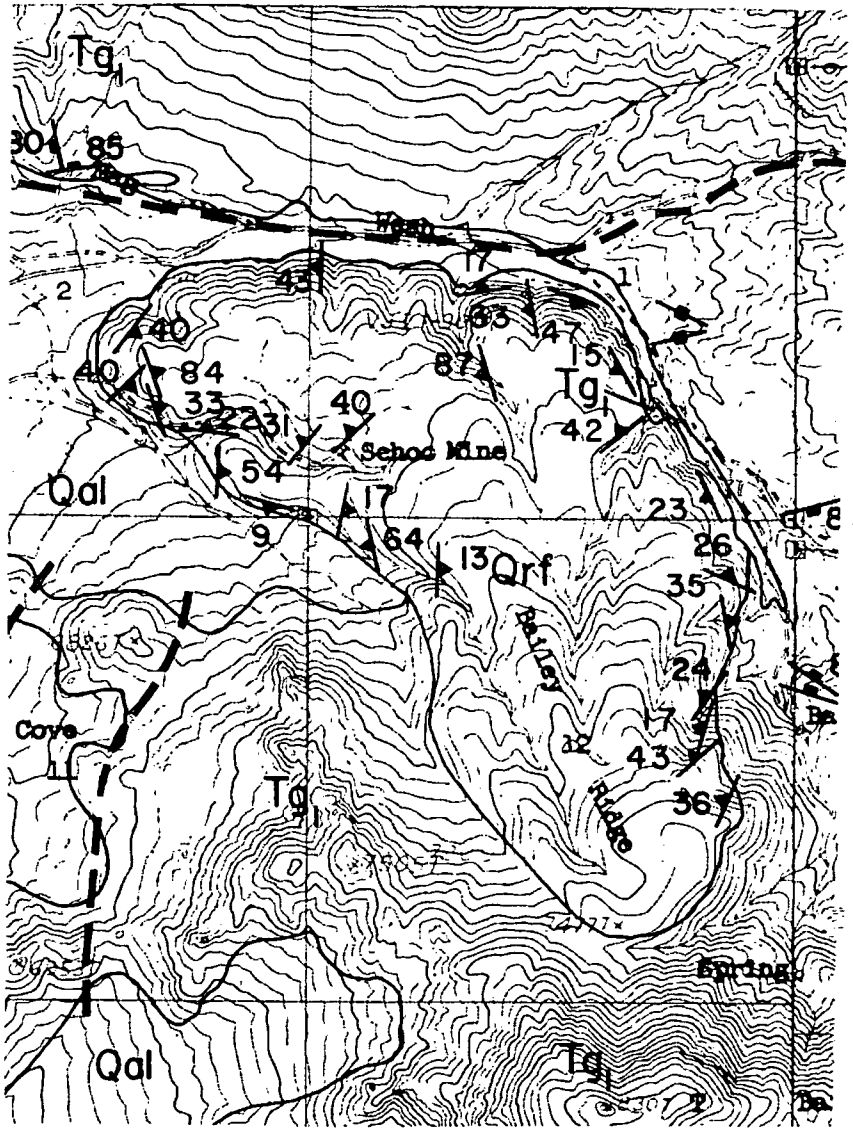

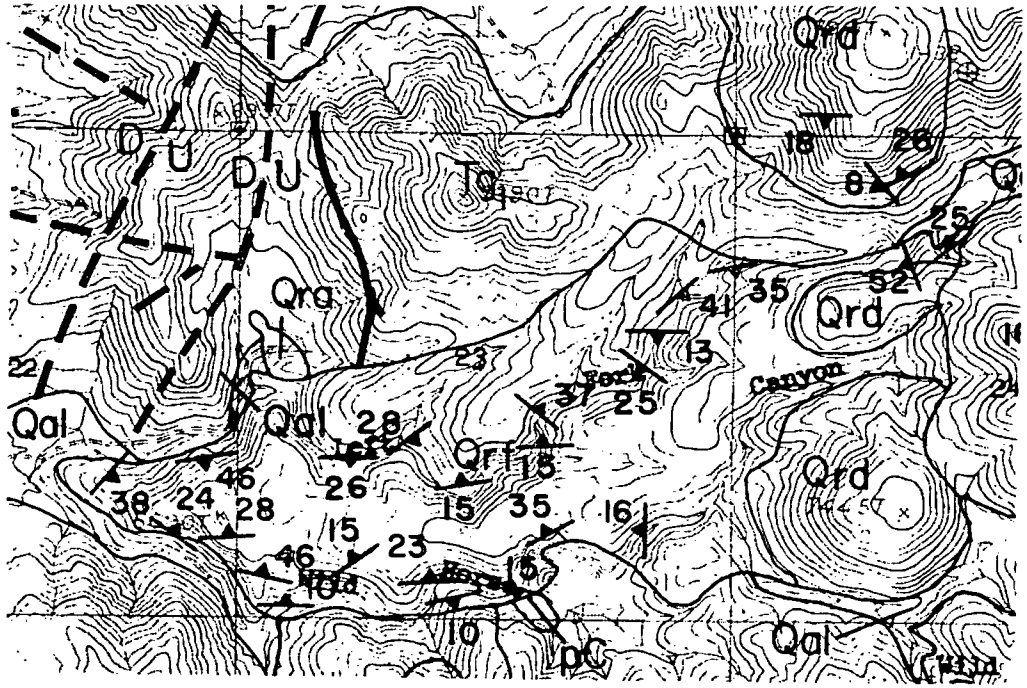

Qal Quaternary alluvium

Qrf Flow layered rhyolite

Qrd Rhyolite domes

Tgl Granite

Qra Ash flow and ash-fall tuffs

pC Precambrian (?) Gneiss

1 0 5 1 KILOMETER

to the flow direction. Lipman et al. (1977) concluded that the flows had lower emplacement viscosities than most silicic lava flows as indicated by planar and uncontorted flow layering, the absence of "ramp structures" (Christiansen and Lipman, 1966), subhorizontal layering, and very limited folding. In essence, compared to most rhyolites, the flows are long, thin and uncontorted.

The porphyritic lava domes are up to 500 m in radius with thicknesses of as much as 250 meters. Many are little eroded and are covered by a rubbly, pumiceous carapace. Where dissected, the domes are seen to have a basal vitrophyre 5 to 10 meters thick which grades upward through flow layered obsidian to a gray, divitrified interior. Gas cavities are common throughout the rhyolite bodies. Flow structures in the domes are more typical of rhyolites in general; flow layering is often nearly vertical, highly contorted, and ramp structures are common in the upper portions of the domes.

VOLATILE CONSTITUENTS

Chemical analyses

Analyses of rocks and residual glasses for water, fluorine and chlorine are given in Table 2. Total water was determined by a modified Penfield method, and bulk rock fluorine was determined colorimetrically by the alizarin fluorine blue method. An electron microprobe was used to measure fluorine and chlorine concentrations in glasses which are reported to the nearest 100 ppm. Whole rock Cl was determined by X-ray fluorescence.

Table 2. H_2O, F and Cl contents of silicic lavas (weight percent)

	Sample	Lithology	H_2O^+	H_2O^-	F	Cl (ppm)
Flows						
	73-3A	obsidian	0.12	0.06	0.16	495
	73-3AG*	obsidian	-	-	0.16	600
	74-8	obsidian	0.06	0.06	0.14	475
	74-8G*	obsidian	-	-	0.15	600
Domes						
	74-7	rhyolite	0.02	0.04	0.12	155
	74-16	obsidian	0.26	0.06	0.38	735
	74-16G*	obsidian	-	-	0.25	900
	74-22G*	obsidian	-	-	0.25	600
	75-14	obsidian	0.13	0.01	0.42	565
	75-14G*	obsidian	-	-	0.34	600
	75-18G*	obsidian	-	-	0.33	800
	75-19	rhyolite	0.18	0.04	0.35	-
	75-20	obsidian	0.10	n.d.	0.44	605
	75-20G*	obsidian	-	-	0.33	700
	74-19	pumice	3.11	0.89	0.26	675

*microprobe analysis of glass (Cl values reported to nearest 100 ppm)

n.d. = not detected

- = not determined

Water contents of obsidian are all less than 0.2 percent, whereas hydrated obsidians (pumice) contain up to 4 percent total water. In fresh samples, fluorine exceeds water with F/H_2O ratios as great as 4 in dome obsidians. Chlorine ranges from 0.05 percent in flows to 0.09 percent in domes.

Fluorine contents of dome-forming rhyolites are higher for the whole rock than for the glass. This is attributed to the presence of phenocrysts of biotite which contain 2.6 to 3.5 percent fluorine (Evans and Nash, 1978). The overall fluorine content of these lavas is high, a characteristic of many rhyolites from the western United States, and is demonstrated by the presence of fluortopaz as a vapor phase deposit in gas cavities in the domal rhyolites. Noble et al. (1967) report values of 0.17 to 0.18 percent F in alkaline rhyolite glasses, while much larger values are attained in peralkaline rhyolites (1.1 - 1.4%). The mean F content of typical rhyolites from the western U.S. is 0.5 percent (Powers, 1961; Coats et al., 1963).

Chlorine contents are 100-200 ppm higher in dome rhyolites than in flows. Both fluorine and chlorine are less abundant in the more crystalline rhyolite (74-7) and presumably were lost during crystallization. Hydrated pumice (74-19), which contains over 4 percent water, shows no significant depletion in either halogen when compared to obsidians of similar bulk composition.

Water fugacity

The fugacity of water in a magma containing biotite, alkali feldspar

and magnetite, may be calculated from the following equilibrium relationship as determined by Wones and Eugster (1965).

$$KAlSi_3O_8 + Fe_3O_4 + H_2O = KFe_3AlSi_3O_{10}(OH)_2 + 1/2\ O_2 \qquad (1)$$

sanidine magnetite annite

The fugacity of water is given by

$$\ln f_{H_2O} = \frac{\Delta G_1^o}{RT} + \ln \frac{(fo_2)^{1/2}(a_{ann}^{bi})}{(a_{san}^{fs})\ (a_{mt}^{sp})}$$

where a denotes the activity of the subscripted component (annite, sanidine, magnetite) in the superscripted phase (biotite, feldspar, spinel). Specific water fugacities were calculated as follows:

$$\log f_{H_2O} = \frac{8673}{T} + 2.46 + 0.5 \log f_{O_2} + 3 \log X_{ann}^{bi} + 2 \log X_{OH}^{bi} - \log a_{san}^{fs} - \log X_{mi}^{sp} \qquad (2)$$

where X is the mole fraction of the subscripted component. The X_{OH}^{bi} term takes into account an assumed ideal entropy of mixing of fluorine in the OH^- site in biotite. Magnetite activities are assumed to be equal to mole fraction, and sanidine activities have been calculated from the relationships of Waldbaum and Thompson (1969). The activity of annite is equal to the cube of the atom fraction of Fe^{2+} (Wones, 1972). The mineral analytical data are taken from Evans and Nash (1978), and temperatures and oxygen fugacities used in the calculations were determined from coexisting iron-titanium oxides. The free energy function used is that advocated by Hildreth (1977) which is based upon a reevaluation of the experimental data of Wones and Eugster (1965).

The results of the calculations are given in Table 3. Flow rhyolites

Table 3. Chemical and physical parameters of rhyolite magmas, Mineral Mountains, Utah.

Sample	74.3	74.8	74.16	74.19	75.22
T°C	740	780	650	645	735
$-\log f_{O_2}$ (b)	13.6	12.9	16.8	16.9	14.3
$X^{biotite}_{annite}$	0.39	0.38	0.40	0.41	0.53
$X^{biotite}_{OH}$	0.63	0.63	0.68	0.69	0.57
$X^{feldspar}_{sanidine}$	0.60	0.60	0.60	0.60	0.70
$X^{spinel}_{magnetite}$	0.78	0.83	0.78	0.78	0.69
f_{H_2O} (b)	775	810	155	180	760
P_{H_2O} (b)	960	965	165	190	945
depth (km)	3.6	3.6	0.6	0.7	3.6
f_{HF} (b)	0.49	0.51	0.08	0.09	0.79
X_{H_2O}	0.13	0.13	0.05	0.06	0.14
H_2O wt. %	4.1	4.1	1.5	1.7	4.7
$\log \eta_{dry}$(poise)	12.1	11.6	13.7	14.0	12.3
$\log \eta_{wet}$(poise)	7.1	6.6	11.3	11.2	6.6
ρ_{dry} gm-cm^{-3}	2.32	2.32	2.33	2.33	2.35
ρ_{wet} gm-cm^{-3}	2.14	2.13	2.25	2.25	2.12

have water fugacities of 775 to 810 b, whereas the dome rhyolites have f_{H_2O} values of 155 to 180 b. Because these values are calculated from phenocryst phases, they must represent pre-eruptive fugacities. The differences in water fugacities between the two magma types may be due to differing water contents, as well as total pressures, in an undersaturated environment. The equivalent water saturated pressures for these fugacities are about 960 and 180 b, respectively. If the magmas were saturated with water, and assuming that water pressure did not exceed lithostatic pressure, the equivalent depths are 3.6 and 0.7 km, respectively. The weight percent of water present in each melt has been calculated using the relationship of Nicholls (pers. commun., 1978); water concentrations at these fugacities and temperatures are given in Table 3 and range from 4.1 weight percent H_2O for flow magmas to about 1.6 percent for dome magmas. If the magmas were undersaturated with respect to water then the calculated lithostatic depths would be greater, and the magma water content could be less. Assuming that temperatures and water fugacities are correct, the wter content of the magmas has been calculated at constant temperature and f_{H_2O} as a function of total pressure. Results for a representative flow and dome are shown in Fig. 3, together with the vapor saturation curve for the Harding pegmatite (Burnham and Jahns, 1962). These data serve to illustrate that even these highly evolved silicic magmas reach water saturation only at relatively shallow levels in the earth's crust.

Fig. 3. Calculated water contents of dome and flow magmas as a function of total pressure at constant temperature and water fugacity as given in Table 3. The vapor saturation curve for the Harding pegmatite is shown as a dashed line.

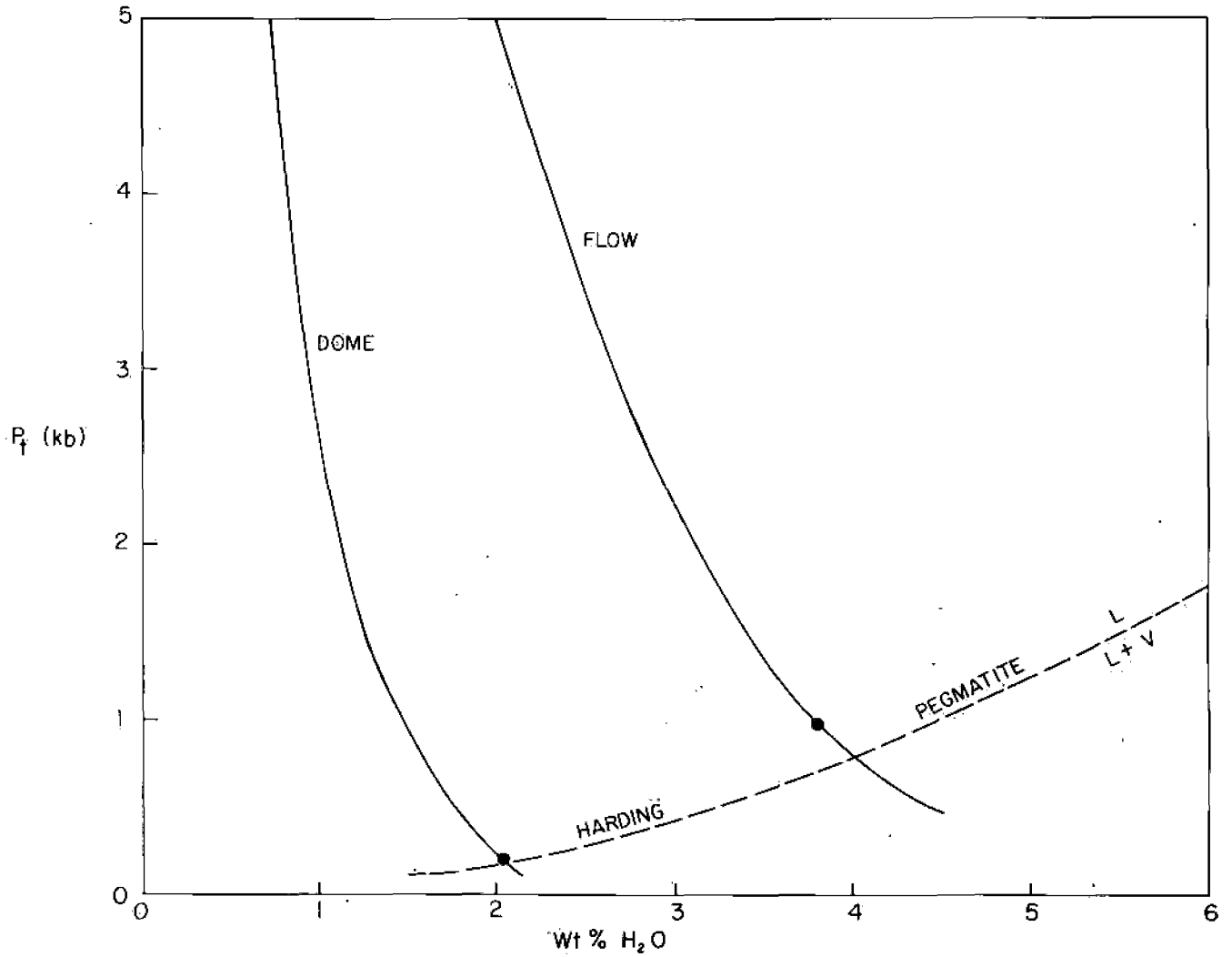
5
4
3
2
1
0
0
1
2
3
4
5
6
P_f (kb)
Wt % H_2O
DOME
FLOW
HARDING
PEGMATITE
L
L + V

HF fugacity

The experimental results of Munoz and Luddington (1974) make it possible to calculate the fugacity ratio f_{H_2O} in the vapor phase, based upon the fluorine content of biotite. The logarithm of the fugacity ratio is similar for both magma types, varying between 3.2 and 3.3. Because f_{H_2O} is known, absolute HF fugacities may be calculated, and they range from 0.5b in flows to 0.08b in domes (Table 3). These results are lower than Kogarko's (1974) estimate that at a water pressure of 1000 atmospheres, the partial pressure of HF in equilibrium with a granite melt would be 2.76 atmospheres.

HF concentrations in magmas

An approximate estimate of HF concentrations in the two magma types can be made by taking the partition coefficient for F between magma and vapor phase to be 0.33 (Burnham, 1967); i.e. one third of the F has been lost to the vapor phase. If so, HF concentrations were between 0.6 and 0.2 weight percent in the dome and flow magmas, respectively. The former is sufficient to lower the experimental solidus by about 20°C (to 650°C) in a water saturated granite melt at 2750b pressure (Wyllie and Tuttle, 1961).

The effect of fluorine on viscosity is not well understood. In their experiments Wyllie and Tuttle (1961) obtained larger albite crystals in melts which contained fluorine than from those with water only; this suggests that viscosities may have been lower in the presence of fluorine, which promoted more rapid diffusion rates. On the other hand, Kogarko and Kugman (1973) concluded that fluorine does not act to depolymerize Si-O

Fig. 4. Viscosity of high-silica rhyolite as a function of water content. Data as shown for temperatures of flow (740°C) and dome (650°C) temperatures.

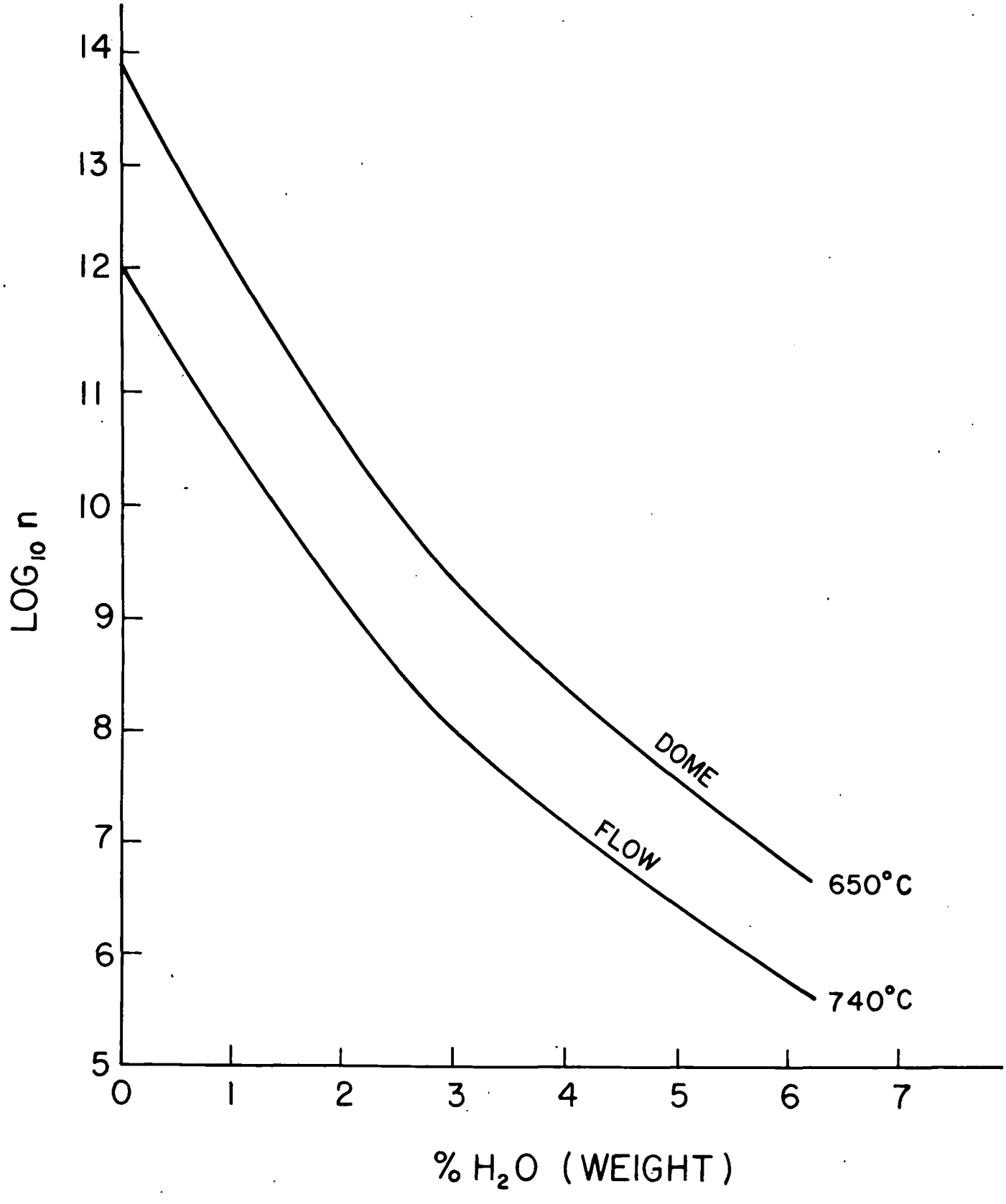
14
13
12
11
10
9
8
7
6
5
LOG10 n
0
1
2
3
4
5
6
7
% H2O (WEIGHT)
DOME
FLOW
650°C
740°C

complexes. If so, we should expect that fluorine does not have a significant effect in reducing viscosities. The matter remains unresolved. We surmise that whether or not either of these conclusions are valid, magma viscosities will not be significantly affected in nature by fluorine due to its overall low concentration. Water content and temperature are the critical factors in the viscosities of most silicic magmas, and we emphasize the fact that the domes of the Mineral Mountains contain up to three times the amount of fluorine as the relatively much more fluid flows.

MAGMA FLUID MECHANICS

Viscosity

The different behavior of flow and dome rhyolite is fundamentally one of differences in the viscosity of each magma type. Magma viscosities have been calculated using the method of Shaw (1972), and we present here a series of calculations to demonstrate the effects of temperature and water content on the viscosity of the magmas at hand (Table 3).

The viscosity of magma as a function of water content for composition 74-3 is shown in Fig. 4. As demonstrated by Shaw (1972), water content has a profound effect on the viscosity of a silicic magma; in passing from anhydrous to water saturated conditions, at constant temperature, the viscosity decreases by a factor of 10^6 poise. Temperature changes do not affect viscosity as strongly. At constant water content a decrease in temperature of 100°C will lower the viscosity by a factor of 10 to 100, depending upon water content.

Flow velocity and estimated water content

Although silicic magmas may contain substantial amounts of water at depth in the crust, it is only reasonable to expect less water to be present as they flow out upon the surface, and that they will continue to expel water during eruption. If the viscosity of the lava at the surface can be estimated, then the water content of the magma at the initiation of flow may be calculated. The average viscosity of a rhyolite flow may be estimated by choosing reasonable limiting values for its flow velocity during eruption.

The velocity of an open channel flow is given by

$$V = \frac{\rho g H^2 \sin\theta}{3\nu} \tag{3}$$

where ρ is the fluid density (2.1 g/cm^3), g is the gravitational constant (980 cm/sec^2), H is the thickness of the flow (80 x 10^2 cm), θ is the average angle from the horizontal (4°), and ν is the viscosity. The actual slope for the flow under consideration is not linear and can be expressed by an equation of the form

$$y = 0.0219\ r^{1.1385} \tag{4}$$

where y is the elevation and r is the distance along the surface of the flow from its terminus. The derivative of equation 4 yields a variation in slope from 3.1° at the terminus to 4.4° at the top. For the purposes of calculation we have assumed a linear slope of 4°. The variation in velocity due to changes in slope is minor compared to that due to changing water content of the magma as shown below.

For flow along a linear slope the numerator is constant, and velocity is simply inversely proportional to viscosity. Fig. 5 shows flow velocity as a function of water content for composition 74-3 at constant temperature (740°C). The isothermal model is adopted as an acceptable approximation because small temperature changes do not alter the viscosity appreciably, and, as shown below, the whole flow would not have cooled significantly while it was in motion. Fig. 5 illustrates that there is an extraordinarily large theoretical velocity range, depending upon water content, from an anhydrous 10^{-4} km/hr to a water saturated 300 km/hr! These are equivalent to emplacement times for a 3 km flow of 125 days to 33 seconds, respectively. More reasonable, but very broad limits are between 10^{-2} km/hr and 1 km/hr, or emplacement times of 300 to 3 hours, respectively; the latter is still quite rapid, but perhaps within the realm of reason because the flow appears to have been very fluid. These limits correspond to water contents of approximately 1 and 3 percent by weight.

A water content between 1 and 3 percent must represent an average value because the magma will be outgassing as it flows, and, as the analyses show, there is obsidian in the flow with negligible water content. In a simple model for such a rhyolite flow, we have adopted an average water content of 2 weight percent distributed linearly from 4 percent at the vent to 0 percent at the extremity of the flow. The effect of this water distribution on the viscosity and velocity of the flow is shown in Fig. 5. As the water content decreases viscosity increases, and the velocity decreases very rapidly until at water contents approaching zero the flow must come almost to a halt. The velocity distribution may be

Fig. 5. Rhyolite flow velocity as a function of water content. See text for discussion.

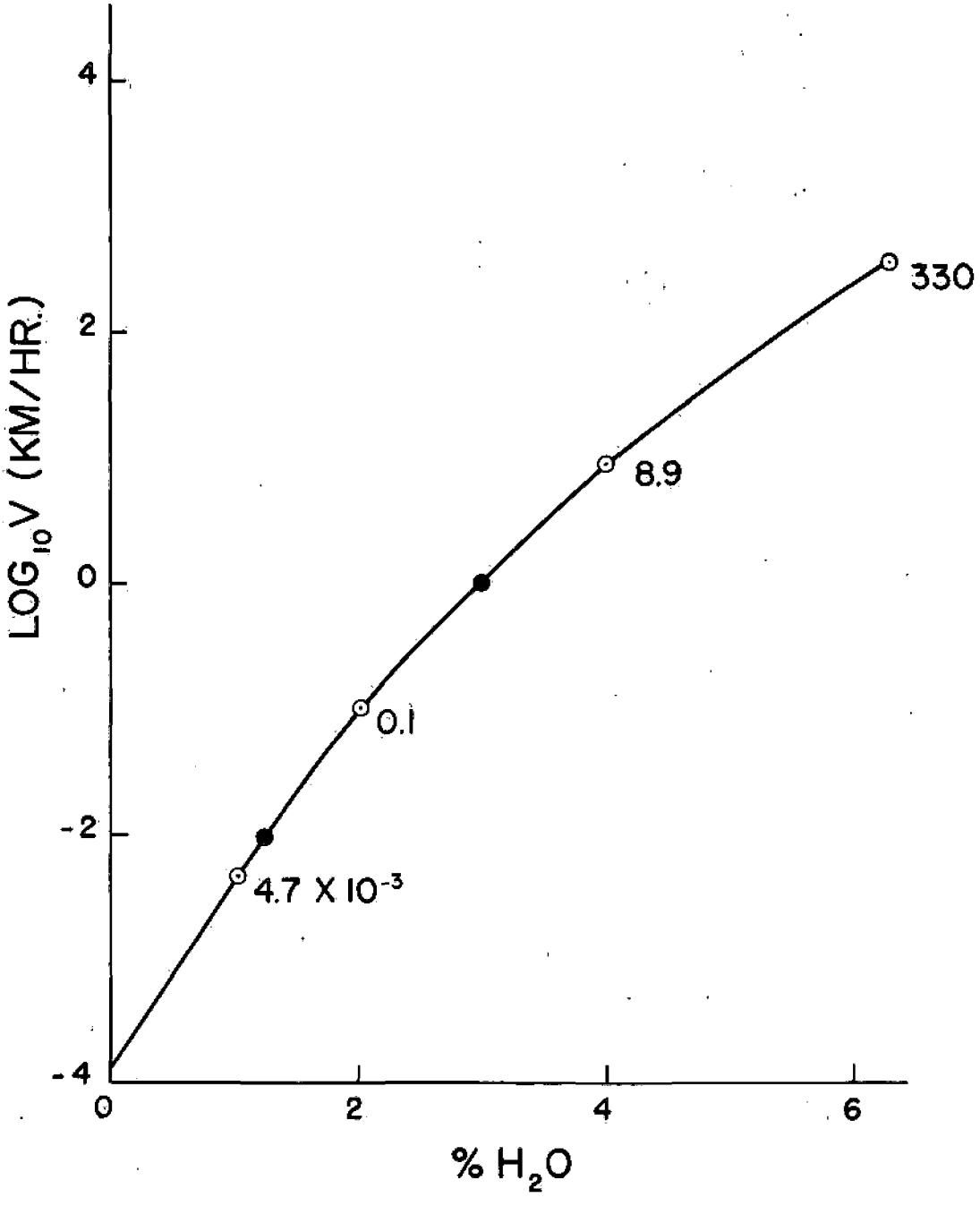
4
2
0
-2
-4
$LOG_{10}V$ (KM/HR.)
330
8.9
0.1
4.7×10^{-3}
0
2
4
6
% H_2O

considered as well to be a profile in time with the velocity dependent upon the rate of volatile loss from the flow. In essence, the model stipulates that rhyolitic magmas when they choose to flow, cease to do so as a result of loss of water. The usual behavior of a rhyolite during extrusion is to resist flow, and to form a viscous dome. These more common rhyolite magmas presumably have lost much of their water prior to their emplacement through pyroclastic eruptions which characteristically precede the formation of rhyolite domes.

Temperature effects

Clearly, as the flow proceeds it must cool, and its increased viscosity will tend to retard its flow. Could it be that a flow forms instead of a dome because of higher initial temperatures in the flow (740°C), and that the flow stops when it reaches the approximate temperature of the domes (650°C)? A simple way to assess this possibility is to determine how long it would take the flow at an initial temperature of 740°C to cool to 650°C in its interior. Temperature, as a function of time and depth in the flow, ($T_{(z,t)}$), is given by the steady state conduction equation:

$$T_{(z,t)} = T_i + (T_i - T_o)\ \mathrm{erf}\left(\frac{Z}{\sqrt{4\alpha t}}\right)$$

where the initial temperature T_i is 740°C, and the ambient temperature T_o is 20°C. The depth, Z, is 40 m, and the thermal diffusivity $\alpha = K/\rho c$, where K is the thermal conductivity (5.6×10^{-3} cal/cm sec deg), c the specific heat (0.3 cal/gm deg), an ρ the density (2.1 gm/cm^3); α = 27 m^2/yr. Solving for time, t, gives a period of 12.6 years. Because this is

considerably greater than the time in which the flow must have been in motion, we conclude that cooling effects were not significant in greatly increasing the viscosity of the magma during its flow. This simple model assumes that radiative heat losses are negligible, and that heat transfer to the surface is solely by conduction; i.e., there is no convective heat transfer. The flow must have been essentially laminar as shown by the small Reynolds numbers over the entire viscosity range. The Reynolds number for open channel flow is given by

$$Re = \frac{4\rho VH}{\nu} \tag{5}$$

Substitution of equation 3 for velocity yields

$$Re = \frac{4\rho^2 gH^3 \sin}{3\nu^2} \tag{6}$$

For the flow under consideration the Reynolds number is less than 2×10^3 for viscosities greater than 6.2×10^5 poise which could only be attained at unrealistic water contents for this magma on the surface (>6% H_2O). Accordingly we conclude that the flow regime was laminar, which is in agreement with field observation.

If the flow were emplaced at higher temperatures, its viscosity would be less, and high water contents would not be required to explain the flow morphology. If so, either the temperature calculations are completely in error, or they do not reflect the eruption temperature, but record equilibration at lower temperatures, after flow had ceased.

We have evaluated the temperature determinations in terms of accuracy and relation to the liquidus. Temperatures obtained from coexisting iron-

titanium oxides whose compositions have been determined with an electron microprobe depend upon several assumptions. The method employed to recalculate microprobe analyses, and the components chosen to make up the end-member compositions will lead to slightly different results when the experimental curves of Buddington and Lindsley (1964) are utilized. We present for comparison three methods of temperature calculation, 1) the calculation of Carmichael (1967) who includes minor components (Mg, Mn, Al, Cr, etc.) in the end-member compositions, 2) a calculation which uses only iron, titanium and oxygen in the end-member calculation, and 3) a method proposed by Lindsley (written communication, 1976) which best accounts for the effects of Mg and Mn in experimental runs. The results are shown in Table 4 along with temperatures determined from coexisting oligoclase and sanidine (Stormer, 1975). The general agreement between these methods leads us to have confidence in the temperature determinations.

Secondly, do these temperatures represent eruption or pre-eruption temperatures, or are they the result of equilibration after the flow had been emplaced? Because the mineral data yield water fugacities of 0.9 kb, we suggest that they are pre-eruptive. Moreover, extensive detailed data on Fe-Ti oxide temperatures from the Bishop Tuff (Hildreth, 1977) show no evidence of re-equilibration of oxides after eruption.

In addition, oxides from the Mineral Mountains are unzoned and uniform in composition in each rhyolite. Accordingly, we maintain that the temperatures calculated represent reasonably accurate pre-eruptive values, and that the flows are not emplaced at super-heated temperatures. The amount of superheat required to produce relatively low viscosities at

Table 4. Comparative thermometry (T°C)

	Method				
Sample	1	2	3	4	Lithology
74-3	740	740	740	--	flow obsidian
75-26	750	785	780	--	flow obsidian
74-16	665	650	640	670	dome obsidian
74-19	665	640	630	-	pumice
75-22	740	735	710	725	tertiary rhyolite
75-30	670	660	660	690	tertiary rhyolite

1. Carmichael (1967)
2. Fe, Ti, O end-members
3. Lindsley preferred
4. Two feldspar (Stormer, 1975)

reduced water contents is substantial. For example, at 740°C and 4 percent water, the viscosity of the flow rhyolite would be approximately 2×10^7 poise. At one percent water, the estimated content of the dome-forming magma, the same viscosity is obtained at temperatures in excess of 1000°C. There is no evidence in the phenocryst phases of such an elevated temperature at the time of eruption.

Summary

The flow characteristics, and hence morphology of rhyolite bodies, are primarily due to differences in water content of the magmas at the surface. Fluorine, even when present in substantial amounts, apparently affects fluid behavior to a lesser degree than water content and temperature. Extremely fluid rhyolite magma of the Mineral Mountains contained between one and three percent water upon eruption. Younger, more viscous dome magmas presumably contained less than one percent water, having lost substantial amounts in pyroclastic eruptions which preceded their emplacement.

II Physical Properties of Rhyolite Magmas

The following properties for magmas are presented in tabular form: molar volume, density, heat capacity, gram formula mass, viscosity, thermal conductivity, thermal diffusivity, kinematic viscosity, and coefficient of thermal expansion. In several instances these properties have been calculated for several water contents of the magmas; these are anhydrous and contents of 4.1 and 1.6 weight percent H_2O for flows and domes, respectively, as estimated in Part I of this study. Table 5 is a key to sample lithologies.

DENSITY

Densities have been calculated by the method of Bottinga and Weill (1970), and are set down in Table 6, in the form $\rho = AT + B$ where T is in degrees Kelvin.

MOLAR VOLUME

Molar volumes ($cal\text{-}bar^{-1}$) have been calculated by the method of Bottinga and Weill (1970) and are set down in Table 7 in the form

$V = A + (B \times 10^{-4})T$, where T is in degrees Kelvin.

HEAT CAPACITY

Heat capacities have been calculated from partial molar heat capacity data given in Carmichael et al. (1977) and are presented in Table 8.

Table 5

Mineral Range Volcanics: Key to Analyses

74-2:	obsidian,	Schoo Mine flow.
74-3:	obsidian,	Schoo Mine flow
74-4:	perlite,	Schoo Mine.
74-7:	rhyolite,	Big Cedar Cove.
74-8:	obsidian,	Wild Horse Canyon flow.
74-13:	obsidian,	Schoo Mine flow.
74-16:	obsidian,	Bearskin Mountain.
74-18:	intrusive porphyry,	near radio relay station.
74-19:	pumice,	Pumice Hole Mine.
74-29:	granite,	Pass Road.
75-14:	obsidian,	Little Bearskin Mountain.
75-19	rhyolite,	North Twin Flat Butte.
75-20:	obsidian,	North Twin Flat Butte.
75-22:	rhyolite,	Corral Canyon.

Table 6. Densities of silicate liquids ($gm - cm^{-3}$)

[$\rho = AT + B$, $T = °K$]

	anhydrous		hydrous		
Sample	A x 10^4	B	A x 10^4	B	wt. % H_2O
74-3A	-.89	2.41	-1.40	2.28	4.0
74-4	-.89	2.41			
74-8	-.90	2.41			
74-7	-.88	2.41			
74-16	-.88	2.41	-1.10	2.35	1.6
74-19	-.89	2.41			
74-29	-.84	2.40			
75-14	-.89	2.41			
75-19	-.88	2.41			
75-20	-.88	2.41			
75-22	-.89	2.42	-1.45	2.26	4.7
75-30	-.95	2.46			

Table 7. Molar volumes of anhydrous silicate liquids

$[V = A + (B \times 10^{-4})T \quad (cal\text{-}bar^{-1}),$

where T is in degrees Kelvin].

Sample	A	B
74-3A	0.633	0.265
74-4	0.633	0.262
74-8	0.632	0.265
74-7	0.635	0.261
74-16	0.631	0.260
74-19	0.634	0.264
74-29	0.634	0.248
75-14	0.633	0.262
75-19	0.634	0.259
75-20	0.634	0.261
75-22	0.632	0.261
75-30	0.625	0.272

Table 8. Heat capacity and gram formula mass

Sample	Cp (cal-mole^{-1}-deg^{-1})	Cp (cal-gm^{-1}-deg^{-1})	GFW dry	GFW hydrous	($\%H_2O$)
74-3A	20.89	0.33	63.92	57.25	(4.1)
74-4	19.37	0.30	64.39		
74-8	20.92	0.33	63.87		
74-7	21.08	0.33	64.01		
74-16	20.64	0.33	62.65	59.87	(1.6)
74-19	18.71	0.29	64.54		
74-29	20.97	0.33	64.22		
75-14	20.70	0.32	63.81		
75-19	20.77	0.32	63.90		
75-20	20.74	0.32	63.87		
75-22	20.84	0.32	64.25	55.86	(4.7)
75-30	19.66	0.31	63.94		

GRAM FORMULA MASS

Values are set down in Table 8.

VISCOSITY

Viscosities have been calculated according to the method of Shaw (1972) and are set down in Table 9 in the form

$$\ln \eta = A/T - B$$

where T is in degrees Kelvin. Values are given for the anhydrous liquid and for several values of hydration. The variation of viscosity with water content is discussed in more detail in Part I of this report.

THERMAL CONDUCTIVITY

The thermal conductivity (K) of silicate melts can be crudely modeled by two terms, one for phonon conduction where K_p is inversely proportional to temperature, and a second term for photon (radiative) conduction, where K_r is proportional to the cube of the temperature.

$$K = K_r + K_p = AT^3 + BT^{-1}$$

where A and B are essentially constant for liquids of constant composition and are assumed to be constant for all silicate liquids in the subsequent calculations.

The method of calculation is as follows: each of the individual thermal conductivity curves for natural silicate liquids given by Murase and McBirney(1973) were fit to a cubic polynomial as given above, and the

Table 9. Viscosity (poise).

[ln η= A/T - B, where T = °K]

	anhydrous		hydrous		
Sample	A	B	A	B	(wt. $\%H_2O$)
74-3A	40971.9	12.55	27299.8	10.50	(4.1)
74-4	41108.7	12.57			
74-8	40987.2	12.55			
74-7	41055.5	12.56			
74-16	40664.9	12.50	34071.2	11.51	(1.6)
74-19	41102.9	12.57			
74-29	42134.0	12.72			
75-14	40923.3	12.54			
75-19	41096.0	12.56			
75-20	40969.2	12.55			
75-22	41100.9	12.57	26225.3	10.33	(4.7)
75-30	38275.3	12.14			

constants A and B were evaluated. Values for A and B for each rock were then plotted against silica content for which linear least squares regressions yielded

$$A = [0.3\ (\%SiO_2) - 6.73] \times 10^{-13}$$

$$B = 0.15\ (\%SiO_2) - 7.51.$$

A plot of calculated values of thermal conductivity versus the measured values of Murase and McBirney (1973) is given in Fig. 6. An andesite is the only rock composition for which the model does not predict measured values. It exhibits an apparently enormously large component of phonon conduction at high temperature when compared to the other silicate liquids.

Thermal conductivity values for Mineral Mountains silicate liquids are given in Table 10 in the form

$$K = A \times 10^{-11}\ T^3 + B/T \quad (cal/cm\text{-}sec\text{-}deg)$$

where T is in degrees Kelvin.

THERMAL DIFFUSIVITY

Thermal diffusivites can be calculated from the above data.

$$\alpha = K/\ \times C_p \quad (cm^2/sec)$$

Values for representative flow and dome rhyolites are given in Table 11 as a function of temperature.

Fig. 6. Calculated versus measured values for thermal conductivity of natural silicate liquids. Experimental data are from Murase and McBirney (1973). (Values in cal/cm-sec-deg $x10^3$)

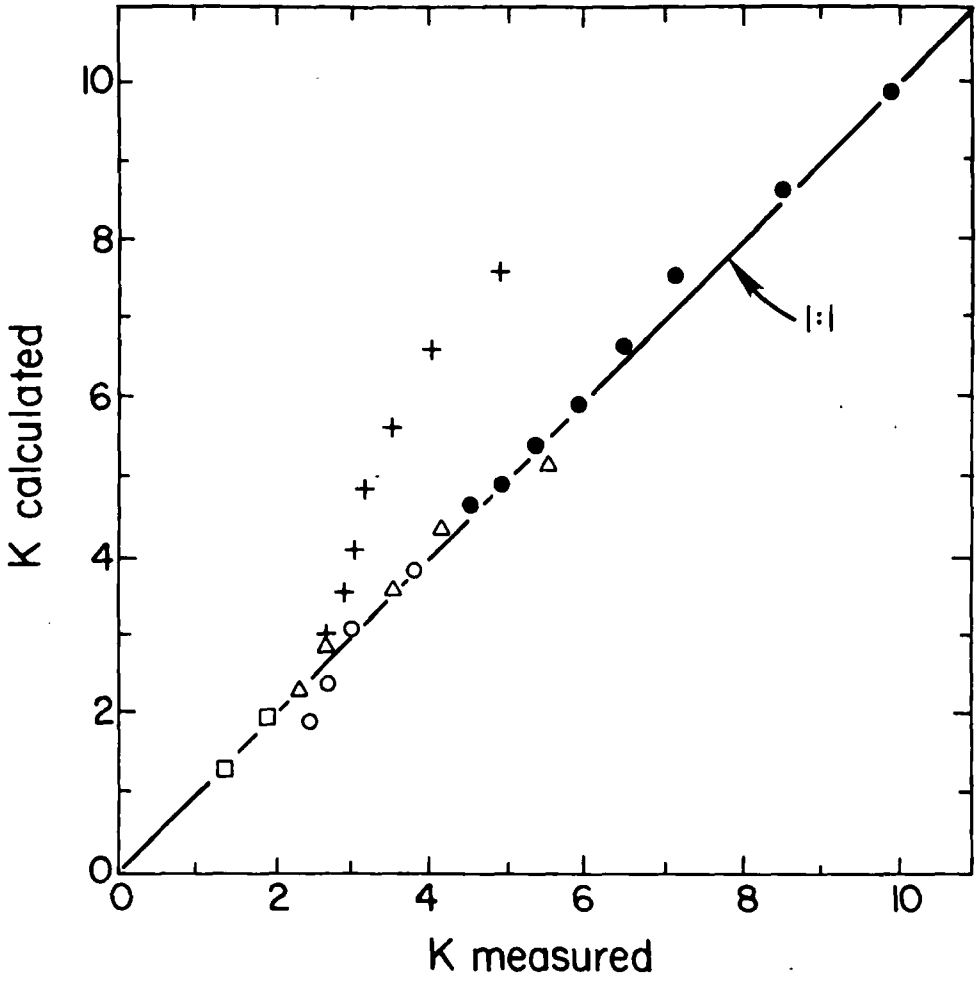

● NRO (obsidian)
○ GOB (olivine basalt)
△ CRB (tholeiitic basalt)
+ MHA (andesite)
□ SLS (lunar basalt)

Table 10. Thermal conductivity of silicate liquids (cal/cm - sec-deg K).

$[K = A \times 10^{-11} T^3 + B/T]$

Sample	A	B
74-3A	0.16	3.97
74-4	0.16	3.67
74-8	0.16	3.97
74-7	0.16	4.01
74-16	0.16	3.89
74-19	0.15	3.42
74-29	0.17	4.12
75-14	0.16	3.95
75-19	0.16	3.96
75-20	0.16	3.96
75-22	0.16	3.89
75-30	0.14	3.01

Table 11. Thermal diffusivity (α), kinematic viscosity (ν), and coefficient of thermal expansion (β) for representative flow (74-3A) and dome (74-16) rhyolite compositions as functions of temperature.

	α ($\times 10^3$)		ν		β ($\times 10^4$)	
T°C	74-3A	74-16	74-3A	74-16	74-3A	74-16
700	7.25	7.07	$.29 \times 10^{13}$	$.22 \times 10^{13}$	.402	.397
800	7.45	7.27	$.58 \times 10^{11}$	$.46 \times 10^{11}$	.400	.395
900	7.87	7.68	$.22 \times 10^{10}$	$.18 \times 10^{10}$	.399	.394
1000	8.51	6.32	$.14 \times 10^{9}$	$.12 \times 10^{9}$	.397	.392
1100	9.37	9.16	$.14 \times 10^{8}$	$.12 \times 10^{8}$	.396	.391
1200	10.46	10.23	$.18 \times 10^{7}$	$.16 \times 10^{7}$	.394	.389

KINEMATIC VISCOSITY

The kinematic viscosity is derived from prior data.

$$\nu = \eta/\rho \quad \text{(Stokes)}$$

Values are tabulated in Table 11.

COEFFICIENT OF THERMAL EXPANSION

The coefficient of thermal expansion, , for silicate liquids is derived from the molar volume data.

$$\beta = 1/V \, (dV/dT)_p \quad (deg^{-1})$$

where V is the molar volume, and T is in degrees Kelvin. Calculated values are set down in Table 11.

REFERENCES

Bottinga, Y. and Weill, D. F., 1970, Densities of liquid silicate systems calculated from partial molar volumes of oxide components. Am. Jour. Sci., 269, 169-182.

Buddington, A. R., and Lindsley, D. H., 1964, Iron-titanium oxide minerals and synthetic equivalents: J. Petrol., v. 5, p. 310-357.

Carmichael, I. S. E., Nicholls, J., Spera, F. J., Wood, B. J., and Nelson, S. A., 1977. High-temperature properties of silicate liquids: applications to the equilibrium and ascent of basic magma. Phil. Trans. Roy. Soc. London, A. 286, 373-431.

Christiansen, R. L. and Lipman, P. W., 1965, Emplacement and thermal history of a rhyolite lava flow near Fortymile Canyon, southern Nevada. Geol. Soc. Amer. Bull., 77, 671-684.

Coats, R. R., Goss, W. D., and Rader, L. F., 1963. Distribution of fluorine in unaltered silicic volcanic rocks of the western conterminous United States. Econ. Geol., 58, 941-951.

Evans, S. H., Jr., 1977, Geologic map of the central and northern Mineral Mountains, Utah. Dept. Geol. Geophys. Report 77-7, Univ. Utah.

Evans, S. H., Jr., and Nash, W. P., 1978, Quaternary rhyolite from the Mineral Mountains, Utah, U.S.A.,(ms.).

Hildreth, E. W., 1977, The magma chamber of the Bishop Tuff: gradients in temperature, pressure and composition. Ph.D. thesis, Univ. Calif., Berkeley, 328 p.

Kogarko, L. N., 1974, Role of volatiles, in: The alkaline rocks, ed. H. Sorensen. John Wiley, 474-487.

Lipman, P. W., Rowley, P. D., Mehnert, H., Evans, S. H., Nash, W. P., and Brown, F. H., 1977. Pleistocene rhyolite of the Mineral Mountains, Utah: geothermal and archeological significance, Jour. Res. U. S. Geol. Surv., 6, 133-147.

Murase, T. and McBirney, A. R., 1973, Properties of some common igneous rocks and their melts at high temperatures. Bull. Geol. Soc. Amer., 84, 3563-3592.

Noble, D. C., Smith, V. C., and Peck, L. C., 1967, Loss of halogens from crystallized and glassy silicic volcanic rocks. Geochim. Cosmochim. Acta, 31, 215-223.

Shaw, H. R., 1972, Viscosities of magmatic silicate liquids: an empirical method of prediction. Am. J. Sci., 272, 870-893.

Stormer, J. C., 1975, A practical two-feldspar thermometer, Am. Mineral., v. 60, p. 667-674.

Ward, S. H., Parry, W. T., Nash, W. P., Sill, W. R., Cook, K. L., Smith, R. B., Chapman, D. S., Brown, F. H., Whelan, J. H., and Bowman, J. R., 1978, A summary of the geology, geochemistry, and geophysics of the Roosevelt Hot Springs thermal area, Utah. Geophysics, in press.

Wones, D. R., 1972, Stability of biotite; a reply, Amer. Mineral, v. 57, p. 316.

Wones, D. R., and Eugster, H. P., 1965, Stability of biotite: experiment, theory and application, Am. Mineral., 50, 1228-1272.